

## Evaluating the dispersibility of rGO prepared using a solvothermal method with DMF and its application as a CDI electrode material: recovery of sp<sup>2</sup>-hybridized carbon

Junho Lee, Seonghyeon Ju, Chaehwi Lim, Jihoon Lee, and Yeojoon Yoon\*

### S 1. Preparation of CDI system

#### S 1.1. Preparation of electrode

The slurry was produced through a sequence of dry mixing, wet mixing, and binder integration processes. Electrodes based on AC, prevalent in many applications, were fabricated by uniformly blending 96 wt.% AC with components such as a solvent, carboxymethyl cellulose (CMC), and styrene butadiene rubber (SBR). Two variants of rGO, each processed by a distinct reduction method, were similarly integrated into the electrode materials, constituting 9.6 wt.% of the mixture other alongside the electrode materials. This slurry was subsequently applied onto a metal sheet at a thickness of approximately 150 μm and dried at 60°C for 2 h. The sheet was subsequently sectioned into squares of 10 cm × 10 cm. The resultant electrodes are depicted in **Figure S 1**.

#### S 1.2. CDI cell assembly and deionization efficiency

The cathode and anode were fabricated using the rGO-based electrodes. The CDI cells were assembled in sequence: cathode, anion exchange membrane, space separator, cation exchange membrane, and anode (**Figure S 2**). The deionization efficiency was evaluated by measuring the conductivity of a NaCl solution with an initial concentration of 2,000 mg L<sup>-1</sup> and conductivity of 4,000 μS cm<sup>-1</sup> before and after passage through the CDI cell at a flow rate of 20 mL min<sup>-1</sup> (**Figure S 3**). Voltages of 1.5 V and -1.5 V were applied for 5 min during the charging phase and for 5 min during discharging, respectively, in a cyclic manner. The conductivity of the effluent was subsequently measured.

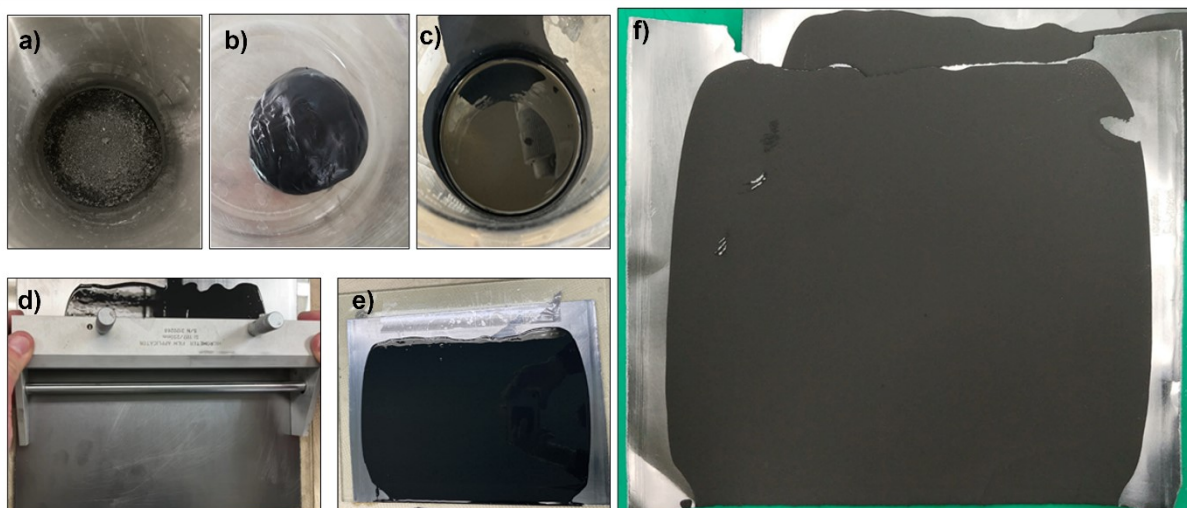


**Figure S 1. Electrode fabrication process. a) Dry mix with activated carbon and rGO. b) Wet mix with binder. c) Wet mix with another electrode materials. d) Slurry coating using doctor blading method. e) rGO-based electrode coated on stainless steel plate. f) Dried electrode.**

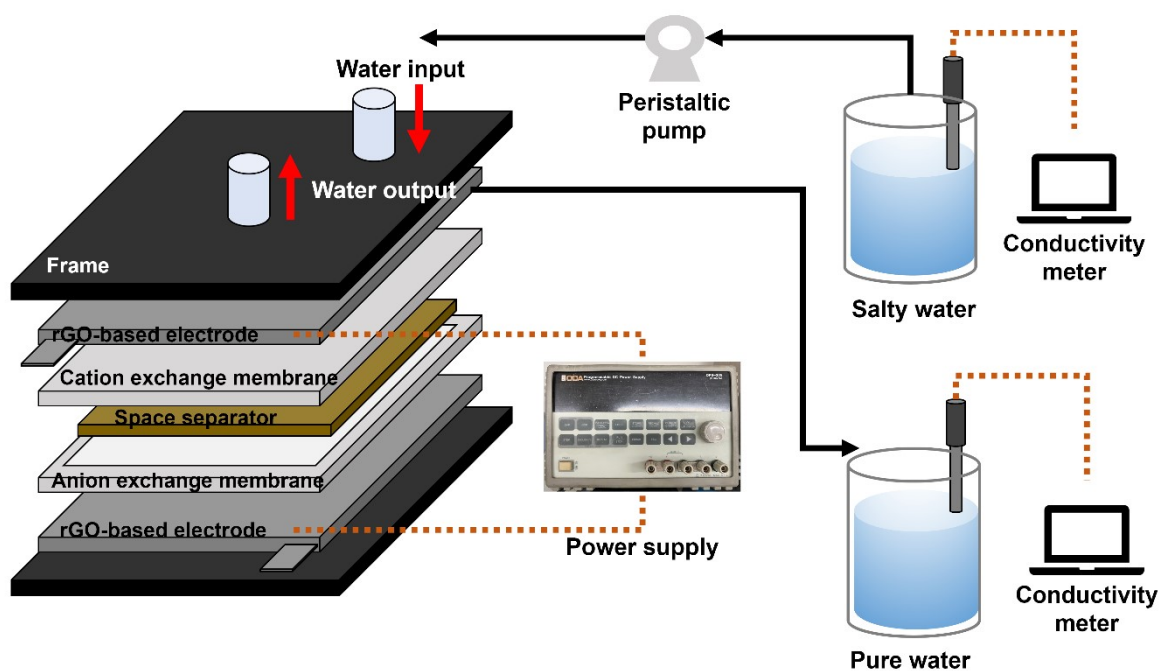


**Figure S 2. Schematic of a single stacked CDI cell used to evaluate deionization efficiency.**

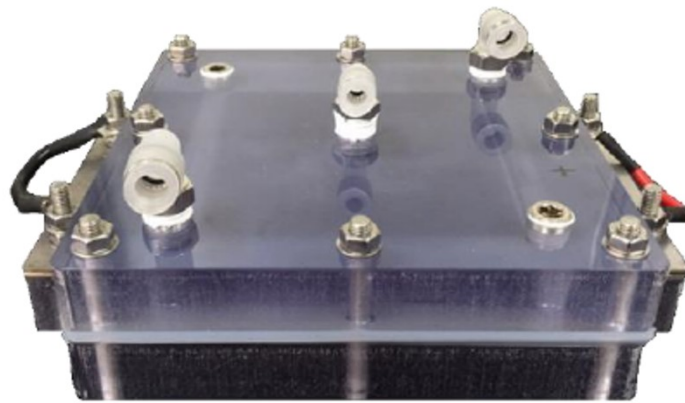


**Figure S 3. Single stack CDI cell.**

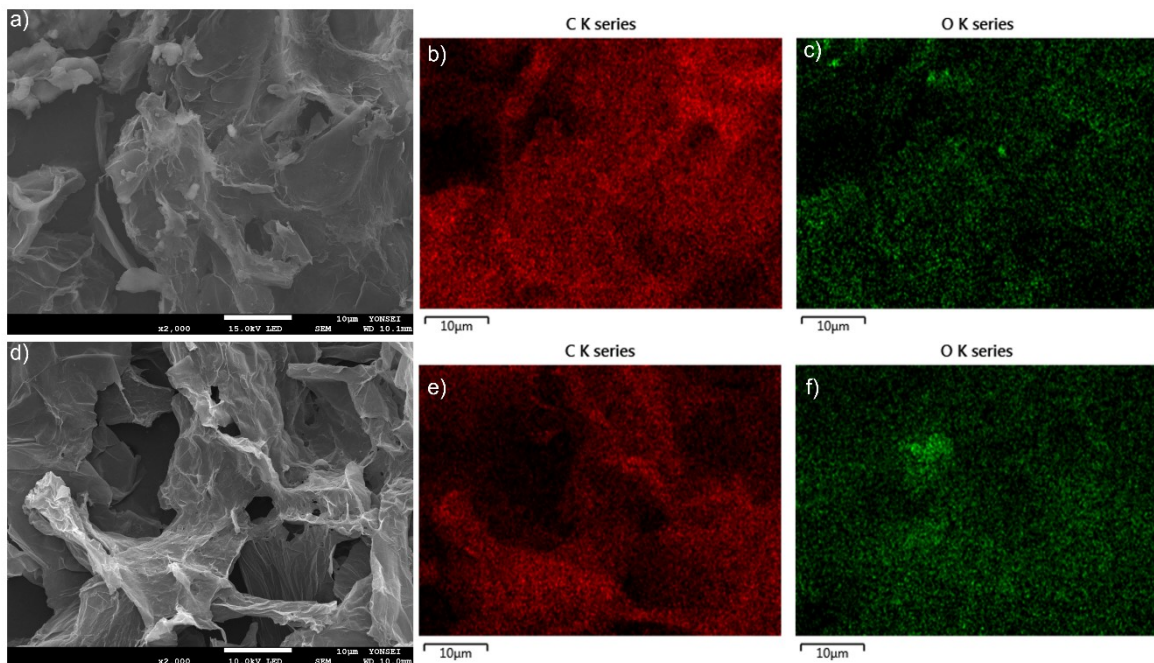


**Figure S 4. FE-SEM image of rGO-D and rGO-H. a) image of rGO-D. d) image of rGO-H. EDS map of carbon b) rGO-D. e) rGO-H. EDS map of oxygen c) rGO-D. f) rGO-H.**

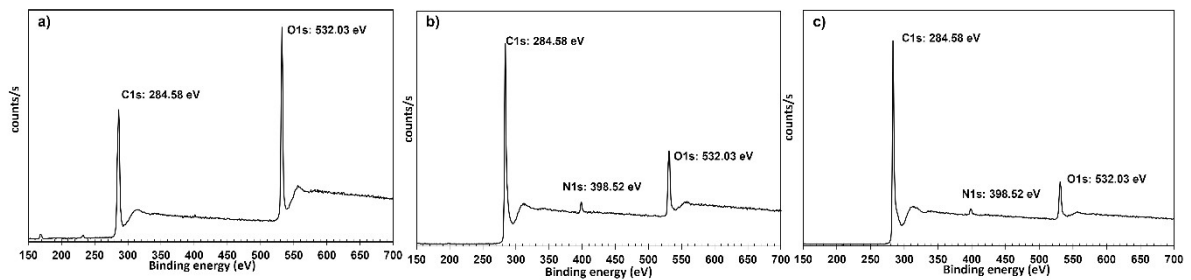


**Figure S 5. C1s, O1s, and N1s XPS spectra. a) GO. b) rGO-D. c) rGO-H.**

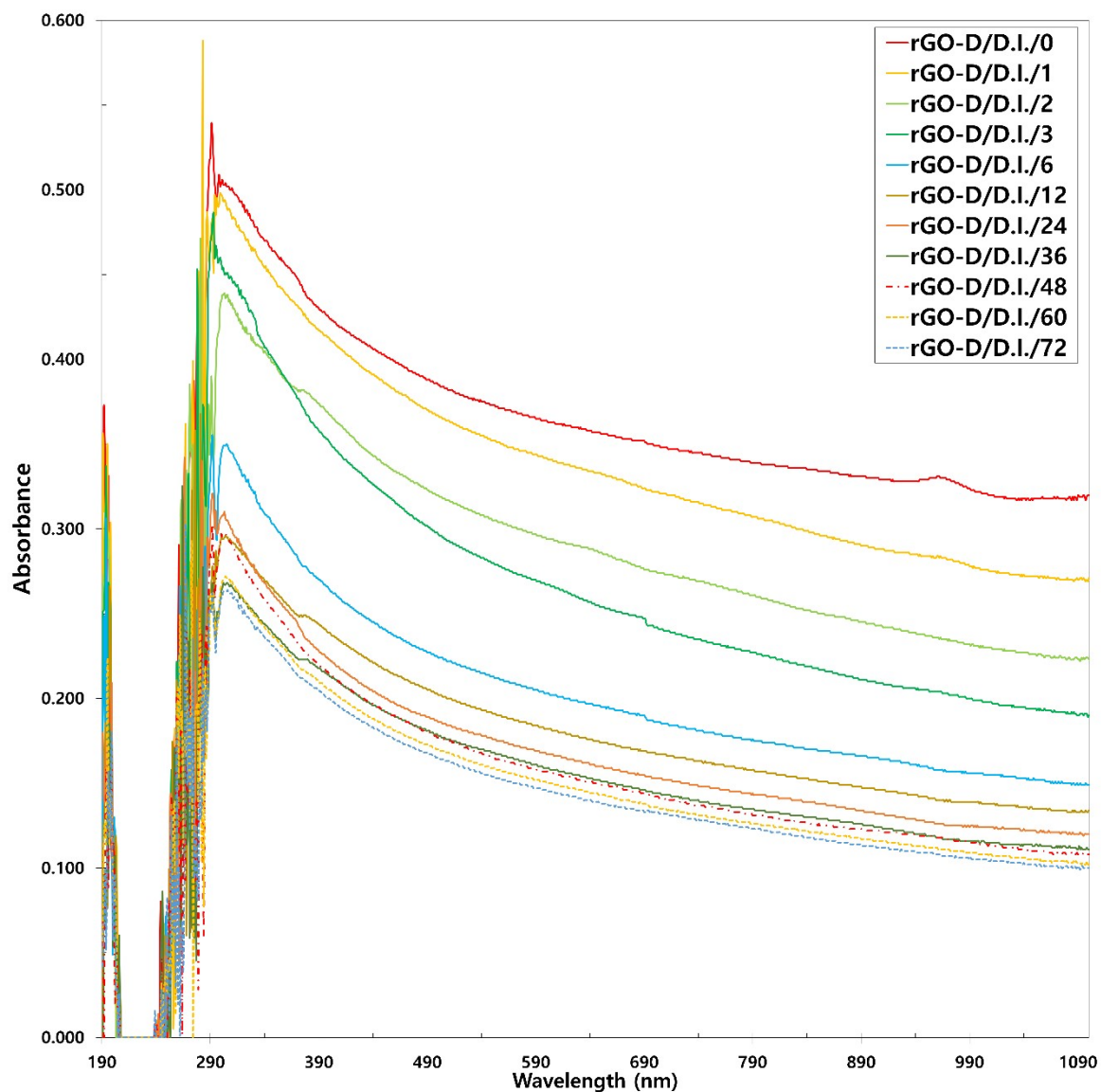


Figure S 6. UV-vis absorbance of rGO-D over time after sonication in D.I. water.

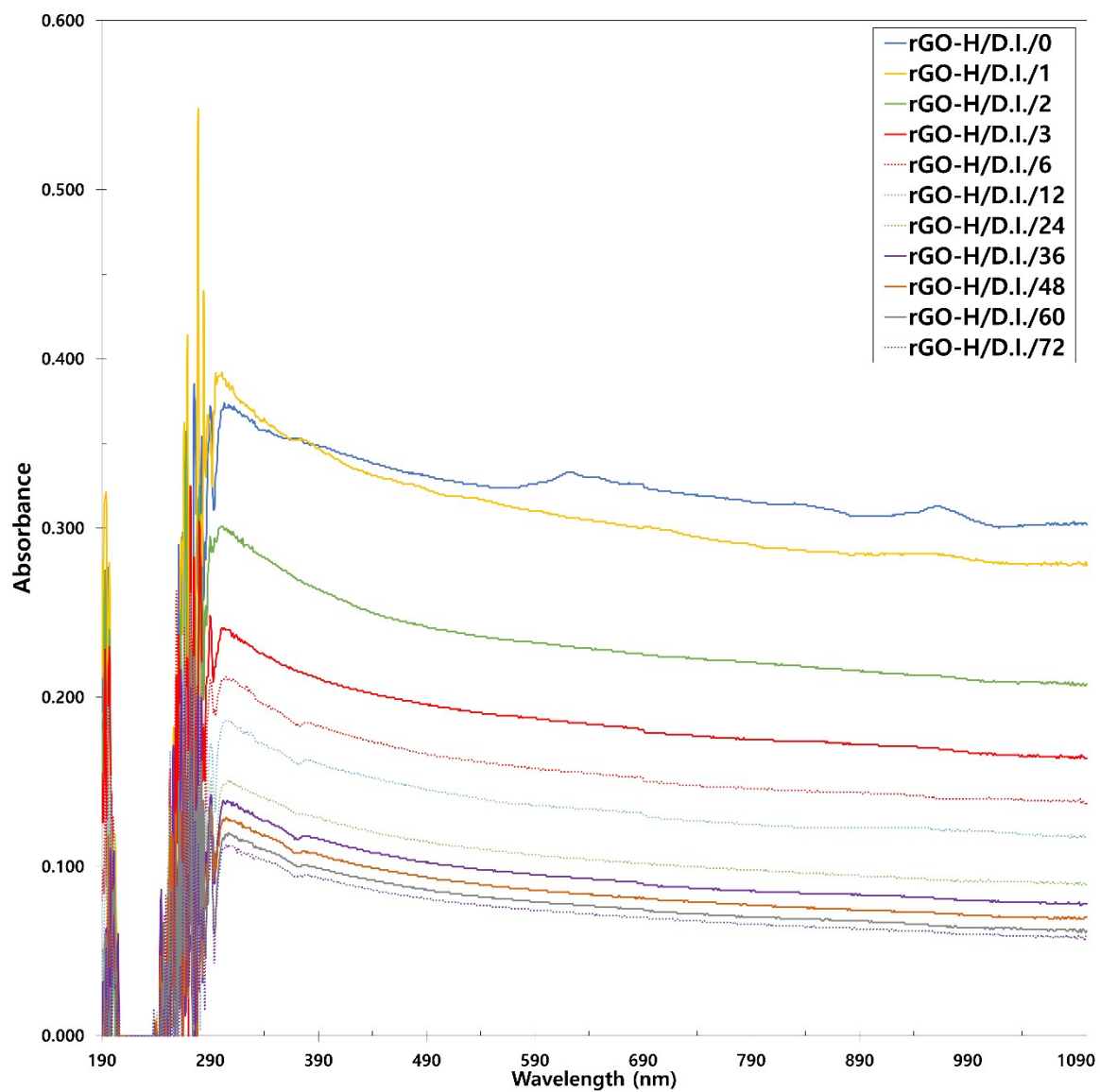
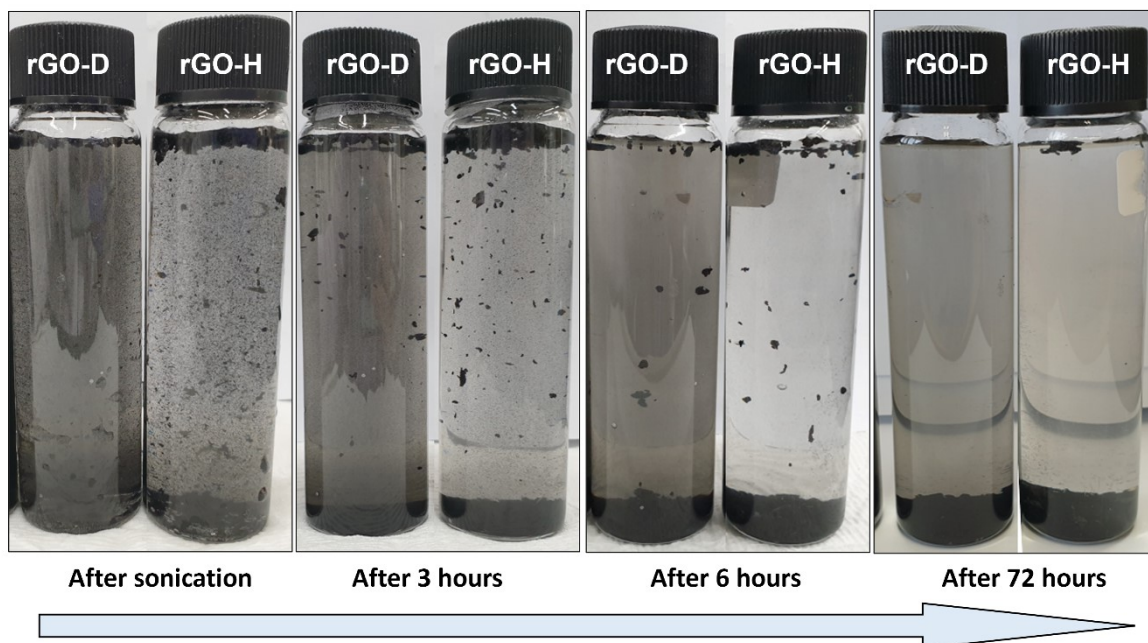


Figure S 7. UV-vis absorbance of rGO-D over time after sonication in D.I. water.



**Figure S 8.** Images showing the changes in rGO-D and rGO-H after sonication in D.I. water

**Table S 1.** Intensity of Raman spectra at D-bands and G-bands of graphene materials. a) Graphite; b) GO; c) rGO-H; d) rGO-D.

	Max $I_D$	Max $I_G$	Peak $I_D$	Peak $I_G$	$I_D/I_G$
a) Graphite	1391	55272	1354.263	1579.273	0.025
b) GO	44386	43790	1350.416	1581.132	1.014
c) rGO-H	58231	58199	1350.416	1579.273	1.001
d) rGO-D	41875	37358	1350.416	1581.132	1.121

**Table S 2.** pH in D.I. water and Zeta potential analysis and Instability Index by LumiSizer. a) rGO-D; b) rGO-H.

Type of rGO	pH	Zeta potential (mV)	Instability Index
a) rGO-D	6.08	-32.22	0.96
b) rGO-H	5.57	-26.35	1.34

**Table S 3. Specific capacitance of materials at 10 cycle**

Materials	Area from CV (mC)	Specific capacitance (F g <sup>-1</sup> ) at 10 cycle
GO	21.553	89.80
rGO-D	42.535	177.23
rGO-H	43.378	180.74
AC	38.653	161.05
AC@GO	26.891	112.05
AC@rGO-D	30.841	128.50
AC@rGO-H	36.728	153.03